GOCE DELCEV UNIVERSITY - STIP
FACULTY OF COMPUTER SCIENCE

The journal is indexed in
EBSCO

ISSN 2545-4803 on line
DOI: 10.46763/BJAMI

BALKAN JOURNAL OF APPLIED MATHEMATICS AND INFORMATICS (BJAMI)

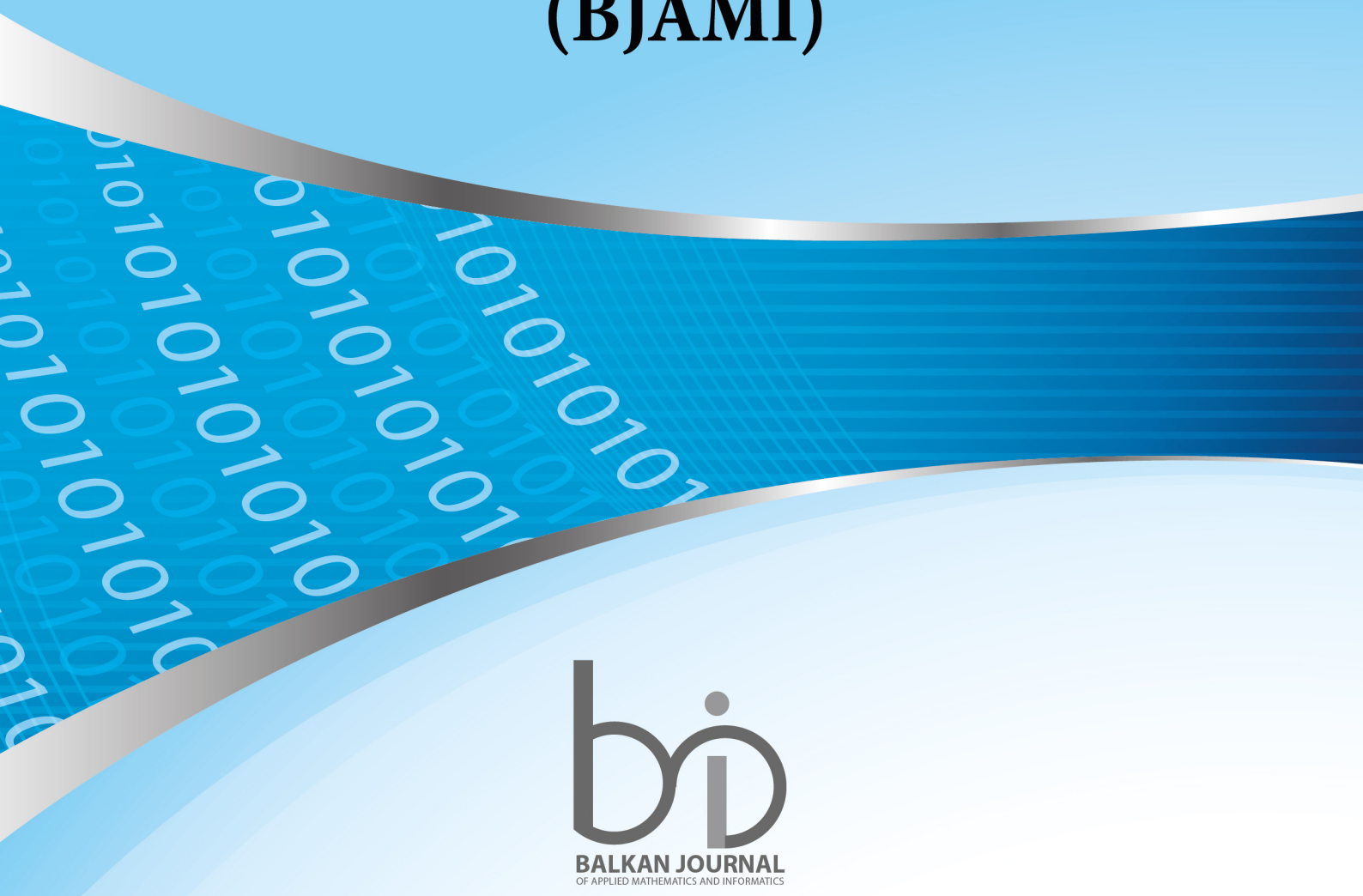

BALKAN JOURNAL
OF APPLIED MATHEMATICS AND INFORMATICS

YEAR 2022

VOLUME V, Number 1

GOCE DELCEV UNIVERSITY - STIP
FACULTY OF COMPUTER SCIENCE

ISSN 2545-4803 on line

BALKAN JOURNAL OF APPLIED MATHEMATICS AND INFORMATICS

(BJAMI)

YEAR 2022 VOLUME V, Number 1

AIMS AND SCOPE:
BJAMI publishes original research articles in the areas of applied mathematics and informatics.

Topics:
1. Computer science;
2. Computer and software engineering;
3. Information technology;
4. Computer security;
5. Electrical engineering;
6. Telecommunication;
7. Mathematics and its applications;
8. Articles of interdisciplinary of computer and information sciences with education, economics, environmental, health, and engineering.

Address of the editorial office
Goce Delcev University – Stip
Faculty of philology
Krste Misirkov 10-A
PO box 201, 2000 Štip,
Republic of North Macedonia

BALKAN JOURNAL
OF APPLIED MATHEMATICS AND INFORMATICS (BJAMI), Vol 3

ISSN 2545-4803 on line
Vol. 5, No. 1, Year 2022

EDITORIAL BOARD

CONTENT

Balkan Journal of Applied Mathematics and Informatics
Volume V Number 1 Year 2022
Online ISSN 2545-4803
UDC: 624.131.535.042.3:517.988

DEPENDENCE OF INPUT ENERGY FROM THE LEVEL OF GROUND NONLINEARITY

ALEKSANDRA RISTESKA-KAMCHESKI AND VLADO GICEV

Abstract. In this paper we studied the characteristics of the response when different boundary conditions are applied. We analyzed a two-dimensional model of the ground-foundation system (construction) and investigated how the physical-mechanical characteristics (density and propagation velocity) of the constituent elements of the ground-foundation system affected the energy that would enter the building.

1. Introduction

In the field of physical phenomena where the region of interest is infinite, such as the case of the problem of propagation of seismic and other types of waves, the application of a numerical simulation is impossible and unnecessary to perform throughout the region. In this case, the artificial boundaries should be such as to allow the wave to travel freely outside the boundaries of the numerical model. By "free" output we mean as little reflection as possible in the numerically modeled region. On the other hand of the propagation of a wave in an infinite domain, there is a wide field of research that involves the response of elements with finite dimensions to a seismic wave. In this case, the boundaries that limit the elements also exist physically. In the process of numerical simulation, the physical response of the borders of the region should be taken. In most cases, boundary conditions are particularly important for simulating the process in the interior region. Different boundary conditions can give completely different simulation results. With the use of numerical methods one problem can be solved from the initial time to a desired time in all spatial points. The most popular numerical methods for solving partial differential equations are the finite element method and the finite difference method. Typically, the finite element method uses implicit schemes in which unknown quantities at all spatial points are determined simultaneously for each time step by solving a system of linear algebraic equations. Otherwise, more finite difference calculation schemes are explicit, where the solution is determined by the solution of the previous time step and the equations are independent. The final elements as a numerical tool are more convenient than the final differences for modeling complex and irregular models. However, for large-scale problems arising in seismology, for example, explicit schemes are recommended because they are cheaper (they require less computer resources) and easier to implement in numerical algorithms. In the last few decades, with the rapid development of computing machines, researchers have been studying wave phenomena through computer simulations of mathematical models. With these simulations we can predict how the object will respond to seismic excitations. This means determining which locations of the building will have a concentration of stresses and large permanent deformations that can lead to the breakage of the building. In addition to the vulnerability of objects, computer simulations of mathematical models help us to study soil damage.

2. Numerical model

We analyzed a two-dimensional model of a ground-foundation-object system (construction). The interest of this research was how the physical-mechanical characteristics (density and velocity of propagation) of the constituent elements of the ground-foundation-object system affected the energy that would enter the building. Because of that, we neglected the geometric details of the building and the foundation and approximated them with rectangles. The building, the foundation, and the soil (ground) have different physical properties. We assumed that the building and the foundation were linear, and that the soil could suffer nonlinear deformation. The nonlinearity of the soil affects the response of the building to excitation at the base. The excitation is from a half-sinusoidal pulse (Fig. 1), and the angle that occupies the direction of propagation of the wave with the vertical is denoted by θ. It is assumed that all the contacts (interfaces) between the building and the foundation, and the foundation and the soil, remain continuous. The height of the building is H_b, and the width $W_b = 2a$. The propagation velocity of the wave in the building is β_b, and the density of the material from which the building is made is ρ_b. The foundation has a depth h_f, density ρ_f and velocity of propagation of the wave through it β_f. The soil has a density ρ_s and a velocity of wave propagation through it β_s. In our model we took a section of soil with the length $L_m = 10a$ and the width $H_m = 5a$. The depth of the foundation is half the width of the building, $h_f = a$.

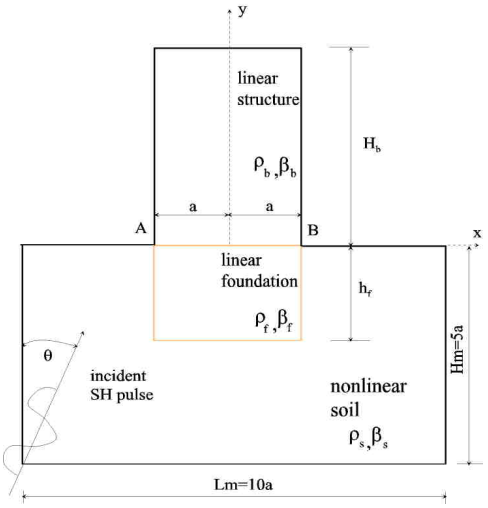

Figure 1. *System with linear structure and foundation and nonlinear soil (Gicev et al, 2015)*

The incoming wave is an SH plane wave in the form of a semisinusoidal pulse and with it we modeled strong impulse movements in the soil. We used the dimensionless frequency $\eta = 2a/\lambda = a/(\beta_s \cdot t_{d0})$ as a measure of the pulse duration, where a is half the width of the base, and $\lambda = \mathrm{T} \cdot \beta_s = 2 \cdot \beta_s \cdot t_{d0}$ is the length of the input wave. $T = 2 \cdot t_{d0}$ is the pulse period, β_s is the propagation velocity of the wave in the soil and t_{d_0} is the pulse duration.

For completeness, we will briefly summarize the model of finite differences and its characteristics. To set the spatial network in the finite difference model, we analyze the pulse in a spatial domain (S) and the displacement at the points obtained because of the pulse is:

$$w(s) = A\sin[(\pi \cdot s / (\beta_s \cdot t_{d0}))] \quad (1)$$

where A is the pulse amplitude and s is the distance from the point under consideration to the front of the wave at the initial time and in the direction of its propagation. Using the fast Fourier transform, the semisinusoid pulse (1) is transformed into a domain of a wave number or spatial frequency (k), as follows:

$$w(k) = F\left[w(s)\right] \quad (2)$$

The maximum response occurs at $k = 0$ (rigid body motion). As it increases k, the answer $w(k)$ decreases (weakens) and approaches zero, approaching k to infinity. Since $\omega = \beta \cdot k$ and $\lambda = 2\pi / k$ with increasing k the angular frequency ω increases and the wavelength λ decreases. For proper discretization of the grid, i.e., correct interval selection, the highest mode must be selected (max k, i.e. min λ) that our grid can reproduce well. In this analysis we chose the maximum wave number, $k = k_{\max}$, for which the answer $w(k)$ is at least 0.03 of the maximum, $w(0)$ (Gicev, 2008). Then, for this value of $k_{\max}$, the corresponding frequencies and wavelengths are:

$$\omega_{\max} = k_{\max}\beta \text{ and } \lambda_{\min} = 2\pi / k_{\max} = 2\pi\beta / \omega_{\max} \quad (3)$$

where $\beta = \beta_S$ is the propagation velocity of the wave in the soil.

The accuracy of the finite difference network depends on the ratio of the numerical and physical propagation velocities, c / β which ideally should be 1. The parameters that affect this accuracy are:

1) The density of the network $m = \lambda / \Delta x$ (m is the number of wavelength points λ, and Δx is the distance between points in the grid);
2) Courant number $\chi = \beta_s \Delta t / \Delta x$ (Δt is a time step);
3) The angle of the input wave θ.

It has been shown that the error increases when m and χ decrease and θ is close to 0 or $\pi / 2$ (Alford et al., 1974; Fah, 1995; Dablain, 1986). For a second order approximation, the above authors state $m = 4$.

To model the soil numerically, we selected a rectangular section with dimensions $L_m = 10a$ and $H_m = L_m/2 = 5a$ (Figure 1). For practical reasons, the maximum number of spatial intervals in the network in the horizontal direction (x-axis) is 200, and in the vertical (y-axis) 400 (125 in the soil plot and 275 in the building). The minimum spatial intervals in the model are $\Delta x_{\min} = L_m / 200 = 76.4 / 200 = 0.382\ m$. For a grid with a smaller spatial interval Δx, the computation time increases rapidly. Thus, for $\eta = 2$, according to the above-mentioned criterion for discretization, the highest mode that we want to be well reproduced with our spatial grid has a wave number $k = k_{\max}$ for which $w(k) \approx 0.03 \cdot w_{max} = 0.03 \cdot w(0)$ has a frequency $\omega_{\max} = 980\ rad / s$.

3. Energy distribution in the system

The flow of energy through a given area can be defined in relation to the passage of the wave through the surface A_{sn}:

$$E_{in}^{a} = \rho_s \cdot \beta_s \cdot A_{sn} \cdot \int_0^{t_{d0}} v^2 \cdot dt \tag{4}$$

Where ρ_s is the density of the soil, β_s is the velocity of propagation of the wave through the soil, v is the velocity of movement of soil particles, and A_{sn} is the area normal to the direction of wave propagation. From the geometry of our calculation model (Figure 1), the area normal to the passing wave is:

$$A_{sn} = 2 \cdot H_m \cdot \sin\gamma + L_m \cdot \cos\gamma = L_m \cdot (\sin\gamma + \cos\gamma) \tag{5}$$

where H_m is the height and L_m width of the soil section in our model (Figure 1), respectively.

By inserting and integrating equations (3) in (2) we get the analytical solution for the wave energy input in the model, as follows:

$$E_{in}^{a} = \rho_s \cdot \beta_s \cdot L_m \cdot (\sin\gamma + \cos\gamma) \cdot (\pi A / t_{d0})^2 \cdot t_{d0} / 2 \tag{6}$$

As can be seen from equation (6), for the defined length of the soil section L_m and the defined input angle γ, the input energy is reciprocal of the pulse duration, which means that it is a linear function of the dimensionless frequency η.

Due to the law of conservation of energy, the input energy is balanced by the following:

- Cumulative energy E_{out} goes out of the model, and is calculated by equation (4),
- Cumulative (hysterical) energy, i.e., the energy consumed for the creation and development of permanent deformations in the soil, is calculated by:

$$E_{hys} = \sum_{t=0}^{T_{end}} \Delta t \cdot \sum_{i=1}^{N} \left(\sigma_{xi} (\Delta\varepsilon_{xpi} + 0.5 \cdot \Delta\varepsilon_{xei}) + \sigma_{yi} (\Delta\varepsilon_{ypi} + 0.5 \cdot \Delta\varepsilon_{yei}) \right), \tag{7}$$

where T_{end} is the time at the end of the analysis, N is the total number of points, σ_{xi}, σ_{yi} are the stresses at points in x and y axis, respectively, $\Delta\varepsilon_{xpi} = \varepsilon_{xpi}^{t+\Delta t} - \varepsilon_{xpi}^{t}$ is the increase of the elastic deformation in the direction x at point i, and $\Delta\varepsilon_{yei} = \varepsilon_{yei}^{t+\Delta t} - \varepsilon_{yei}^{t}$ is the increase of the elastic deformation in the direction y at the point i.

- The instantaneous energy in a building, which consists of kinetic and potential energy, can be calculated from:

$$E_b = E_k + E_p = 0.5 \cdot \Delta x \cdot \Delta y_b \cdot \sum_{i=1}^{N} \left(\rho \cdot v_i^2 + \mu \cdot (\varepsilon_x^2 + \varepsilon_y^2) \right), \tag{8}$$

where Δx and Δy_b are the horizontal and vertical distances of the grid in the building, ρ and μ are the density and shear modulus of the building, respectively, v_i is the velocity of the particles, while ε_x and ε_y are the deformations at point *i* of the building. To study only the effect of scattering on the foundation, it is assumed that the building is high enough that the reflected wave from the top of the building cannot reach the building-foundation contact by the end of the analysis. The analysis is stopped when the wave is completely out of the ground.

4. Numerical example

We took the Holiday Inn Hotel in Van Nuys, California as a prototype for our two-dimensional numerical model (Figure 2). The hotel is located in the middle of the San Fernando Valley in the metropolitan area of Los Angeles, California, and was fully instrumented. During the Northridge earthquake in California in 1994, the hotel was severely damaged (Figure 3) and its response during this earthquake has been analyzed and described in many articles and reports (Li and Jirsa, 1998; Browning et al., 2000); Trifunac and Ivanovic, 2003; Gicev and Trifunac 2006; Gicev and Trifunac 2011. For our two-dimensional SH model, we took the physical-mechanical characteristics of the soil on which the hotel is built, as well as the equivalent physical-mechanical characteristics of the hotel in the east- west, obtained by impulse response analysis of a one-dimensional model.

Figure 2. *View of the hotel "Holiday Inn" Nuys from North-East*

Figure 3. *Post-earthquake view of in Van damaged columns*

We assumed that all contacts in our model, three foundation-soil contacts and one foundation-building contact (Figure 1) remain continuous, i.e., no separation or sliding is allowed. The building and the foundation remain linear throughout the analysis. Figure 1 shows the dimensions of the model and the physical-mechanical characteristics of the elements that make up the model in general numbers. For our example, the propagation velocity of the SH wave in a building is $\beta_b = 100\,m/s$, $\beta_s = 250\,m/s$ in the ground. The width of the foundation is the same as the width of the building $W_b = 2a = 19.1m$, and its depth is half of its width, $h_f = a = 9.55\,m$. The density of the

material from which the building is constructed is $\rho_b = 270\ kg/m^3$ for all examples in this study. We took the density of the foundation and the soil the same $\rho_f = \rho_s = 2000\ kg/m^3$. We stop the calculation at time *Ts*, when the complete filtered pulse passes the right corner of the foundation-structure contact, B (Figure 1).

$$T_s = \frac{H_m}{c_y} + \frac{\frac{L_m}{2} + a}{c_x} + t_d = \frac{H_m}{c_y} + \frac{6a}{c_x} + t_d, \qquad (9)$$

Where $c_y = \frac{\beta_s}{\cos\gamma}$ and $c_x = \frac{\beta_s}{\sin\gamma}$ are the vertical and horizontal phase velocities of the SH wave propagating in the soil, L_m and H_m (Figure 1) are the width and height of the soil section, a is the half-width of the structure and t_d is the duration of the half-sinusoidal pulse. After this time, we have no energy input in the construction. Since we only researched the energy that enters the construction, we varied the height of the building, H_b. We calculated the height of the building from the condition for the time after the wave front (pulse) that reached point A (Figure 1), reached the top of the structure, bounced and continued to travel backwards, did not reach the foundation-building contact until the moment when the complete pulse has passed point B when we interrupt the numerical simulation. The shortest time to reach the wavefront from the lower left corner of the model to the left corner of the foundation contact, then bounce off the top of the structure and reach the foundation contact again is:

$$T_r = \frac{H_m}{c_y} + \frac{\frac{L_m}{2} - a}{c_x} + \frac{2H_b}{\beta_b} = \frac{H_m}{c_y} + \frac{4a}{c_x} + \frac{2H_b}{\beta_b} \qquad (10)$$

Then the required condition for calculating the height of the building is $T_r \geq T_s$, or

$$\frac{H_m}{c_y} + \frac{4a}{c_x} + \frac{2H_b}{\beta_b} \geq \frac{H_m}{c_y} + \frac{6a}{c_x} + t_d \qquad (11)$$

From (11) and keeping in mind that $c_x = \frac{\beta_s}{\sin\gamma}$, we calculate the required height of the structure (object) $H_b \geq \frac{a \cdot \sin\gamma \cdot \beta_b}{\beta_s} + \frac{t_d \cdot \beta_b}{2}$.

From the point of view of design of seismically resistant structures, it is important to know the excitation at the base of the structure. Because the input energy through a given cross-section depends on the velocity of the particles at equation (11), we investigated how different factors affect the velocity of the particles at the foundation-object contact, and thus at the seismic energy entering the building. The factor that we researched was the level of nonlinearity of the ground C, at different input angles θ. For

this purpose, we have defined the mean velocity of the particles of the contact object-foundation:

$$v_{av} = \frac{\sum_{i=1}^{N_c} v_i}{N_c}, \qquad (12)$$

where N_c is the number of points of the contact foundation-object, and v_i is the velocity at point *i* of the contact in time step *k*. In this way, for each time step of our numerical simulation, we calculated the mean pulse excitation velocity with a dimensionless frequency η. For the largest absolute value of the mean velocity and the corresponding η, we obtain a point on the curve $v_{av,\max}(\eta,t)$. We conducted the research in the domain of the dimensionless frequency of excitation $0.06 \le \eta \le 3$ with a step $\Delta\eta = 0.02$. In this way we have $N_p = \frac{3-0.06}{0.02} + 1 = 148$ points on our curves $v_{av}(\eta)$.

5. Results and discussion

Figures 4, 5, 6 and 7 show the normalized curves $v_{av,r}(\eta) = v_{av,\max}(\eta,t)/v_{\max,ff}$, where $v_{\max,ff}(\eta)$ is the highest velocity at absolute value that occurs on the free surface when the foundation and the object would not exist and we calculate how $v_{\max,ff} = 2 \cdot \left| \left(\frac{d_{i+1} - d_i}{\Delta t} \right) \right|_{\max}$, where d_i is the *i*-th order of the filtered seminusoidal pulse. These curves are shown for three degrees of nonlinearity of the ground, at four different input angles, $\theta = 0^0$, 30^0, 60^0 and 85^0. It is obvious that, in Figure 4, $v_{av,r}(\eta)$ for the model of ground with the lowest level of nonlinearity, C = 1.5 (blue line), has the largest ordinates.

For the longest pulses, η = 0.06, has an ordinate one and as η increases to η = 0.48, it decreases. At η = 0.48 the relative mean velocity has a minimum, = 0.89. As η continues to grow, begins to grow slightly and reaches values between 0.92 and 0.93 in the interval. With further growth of η, decreases slightly and at the largest considered value of the dimensionless frequency η = 3 gets a value = 0.89. The soil model with the nonlinearity level C = 1.1 (green line), for the longest pulses, η = 0.06 to η = 0.48, has the same ordinates as the soil model with the nonlinearity level C = 1.5, which has a local minimum at this η. The model with C = 1.1 has a minimum = 0.859 for η = 0.58, and further by increasing η, it goes parallel to the curve with the level of nonlinearity C = 1.5. The maximum $v_{av,r}(\eta)$ = 0.898 occurs at η = 1.2, and $v_{av,r}(\eta)$ = 0.868 for η = 3. The model with the largest nonlinearity on the ground, C = 0.8 (red line), follows the

trend of the previous two curves, by not starting from 1 for the smallest considered dimensionless frequency, η = 0.06, but from $v_{av,r}(\eta)$= 0.8.

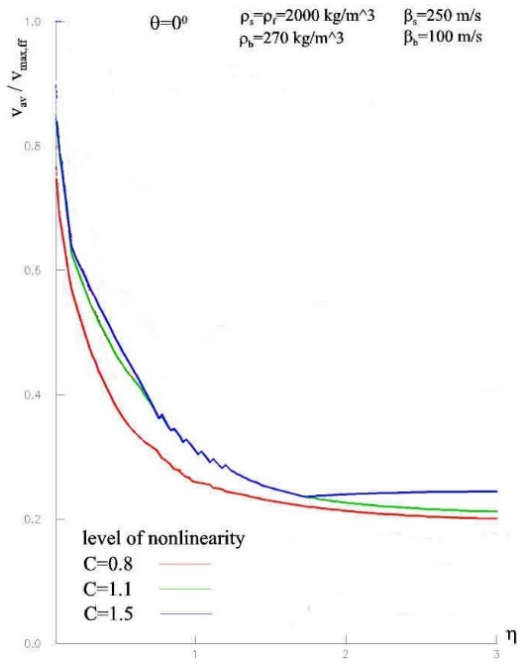

Figure 4. *Peak average velocity v_{av} at structure-foundation interface normalized by peak free-field velocity $v_{max,ff}$ vs. η for three levels of nonlinearity of soil. $\theta = 0^0$*

This is because in the previous two curves, for the smallest dimensionless frequencies, the ground is linear and there is no permanent deformation in it, which is not the case with the model with large nonlinearity, C = 0.8, when permanent deformations occur at the smallest η. Models with low nonlinearity on the ground have larger ordinates than models with higher nonlinearity. The model with the highest level of nonlinearity in the ground C = 0.8 (red line) has the smallest ordinates of $v_{av,r}(\eta)$ for all η, which leads to the conclusion that the models with high nonlinearity in the soil, i.e. small ε_m, i.e. small C in equation (2) prevent (do not allow) much of the energy to reach the object (to the foundation-object contact). This insight allows us to understand why many of the buildings on weak soil (with a high level of nonlinearity) and close to the epicenter of the 1994 Northridge earthquake remained completely undamaged. As the input angle θ increases, for high frequencies (Figures 5 to 7), the curves approach. Figure 5 shows the corresponding input angle curves $\theta=30^0$. As η increases, the curves $v_{av,r}(\eta)$ approach each other.

In Figure 5, it can be seen that for lower nonlinearity, C = 1.1 and C = 1.5 (green and blue lines), the curves $v_{av,r}(\eta)$ almost match, especially at high dimensionless frequencies. Otherwise, for this input angle, $\theta = 30^0$ the curves for large nonlinearity C = 0.8, have different, always smaller ordinates than the curves for C = 1.1 and C = 1.5.

Figure 6 shows the curves $v_{av,r}(\eta)$ for input angle θ = 60^0. The figure shows that for small η the model with the lowest level of nonlinearity on the ground C = 1.5 has the highest value for the average velocity.

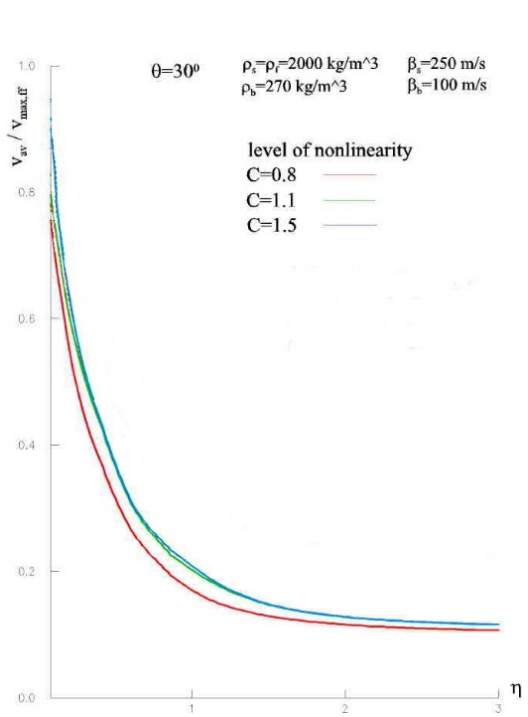

Figure 5. *Same as Fig.4 but for θ = 30^0*

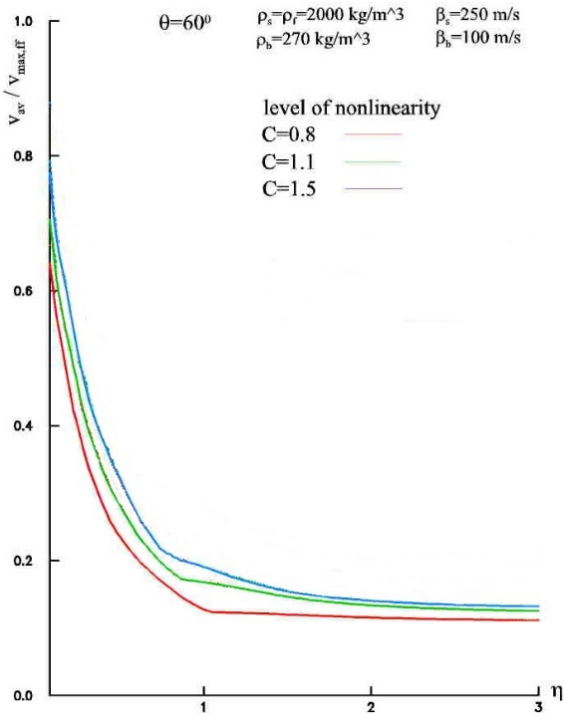

Figure 6. *Same as Fig.4 but for θ = 60^0*

For $\eta = 0$, i.e. for the longest pulses, $v_{av,r}(\eta)$ has the ordinate close to 0.86 and as the dimensionless frequency increases, $v_{av,r}(\eta)$ decreases sharply. At $\eta = 0.5$ the relative velocity of the model with the lowest level of nonlinearity on the ground C = 1.5, it becomes greater than the same for C = 1.5. For $\eta > 0.5$, the relative velocities for this model are the highest and reach the lowest value in the considered interval, about 0.25. The model with the level of nonlinearity on the ground C = 1.1 for $\eta = 0$ has a maximum ordinate for the relative velocity 0.8. The curve of this model runs parallel to the curve with the nonlinearity level C = 1.5 and the minimum occurs for $\eta = 3$, $v_{av,r}(\eta) = 0{,}24$. The model with the largest nonlinearity on the ground (red line) behaves similarly to the previous curve, in that the minimum value for the mean velocity reaches the same for $\eta = 3$, $v_{av,r}(\eta) = 0{,}2$. It is observed that the increase of the input angle leads to the approximation of the curves $v_{av,r}(\eta)$.

Figure 7 shows the curves of the previous mathematical models, but at the input pulse angle θ = 85^0. It is obvious that the maximum value for the relative velocity is lower than that at the input angle θ = 60^0, $v_{av,r}(\eta) = 0{,}75$. This value reaches the curve of the

model for the lowest nonlinearity of the ground C = 1.5 (blue line). The curve with the level of nonlinearity C = 1.1 behaves similarly, with a small difference in the maximum and minimum of the relative velocity. Curves with large nonlinearity on the ground (C = 0.8) have the lowest value for velocity, about 0.58. As η increases, they decrease and for $\eta = 3$ reach the minimum, about 0.1. Figure 7 also shows that as the pulse input angle θ increases, as the frequency increases, the curves $v_{av,r}(\eta)$ decrease and move closer to each other (some of them even coinciding). This shows that at higher η the degree of nonlinearity of the ground is almost irrelevant to the values of the relative velocity of the foundation-object contact, $v_{av,r}(\eta)$. It is also obvious that these velocities for larger η become almost constant, i.e., they no longer depend on the frequency.

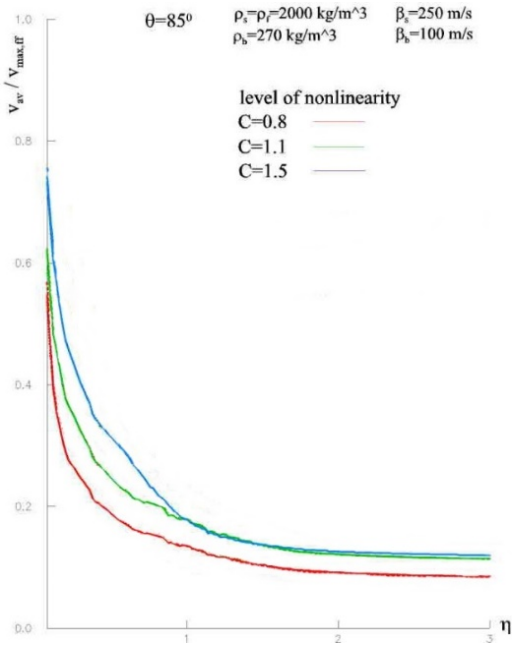

Figure 7. *Same as Fig.4 but for* $\theta = 85^0$

6. Conclusion

We conclude that the models with high nonlinearity on the ground have the smallest ordinates for $v_{av,r}(\eta)$, i.e., as the nonlinearity of the ground increases, so most of the input energy is scattered from the foundation and a smaller part enters the building.

References

[1] *Li, Y.R., and Jirsa, J.O.* (1998). Nonlinear analyses of an instrumented structure damaged in the 1994 Northridge earthquake, *Earthquake Spectra*, *14*(2), 265–283.
[2] *Browning, J.A., Li, R.Y., Lynn, A., and Moehle, J.P.* (2000). Performance assessment for a reinforced concrete frame building. *Earthquake Spectra*, *16*(3), 541–555.
[3] *Trifunac, M.D., and Ivanovic, S.S.* (2003). Analysis of Drifts in a Seven-Story Reinforced

Concrete Structure, *Dept. of Civil Eng. Report No. CE 03-01*, Univ. of Southern California, Los Angeles, California.
[4] *V. Gicev and M.D. Trifunac* (2006). Non-linear earthquake waves in seven-story reinforced concrete hotel, Report CE 06-03
[5] *Gicev, V. and Trifunac, M.D.* Asymmetry of nonlinear soil strains during soil-structure interaction excited by SH pulse, *Izgradnja*, vol. 66, br. 5-6, 2012, 129-148
[6] *Vlado Gicev, Mihailo D. Trifunac, Nebojsa O.* - Translation, torsion, and wave excitation of a building during soil-structure interaction excited by an earthquake SH pulse, Soil Dynamics and Earthquake Engineering, vol. 77, 2015, 391-401.
[7] *Vlado Gicev, Mihailo D. Trifunac, Nebojsa O.* - Two-dimensional translation, rocking, and waves in a building during soil-structure interaction excited by a plane earthquake P-wave pulse, Soil Dynamics and Earthquake Engineering, vol.90, 2016, 454-466.
[8] *Vlado Gicev, Mihailo D. Trifunac, Nebojsa O.* - Two-dimensional translation, rocking, and waves in a building during soil-structure interaction excited by a plane earthquake SH-wave pulse, Soil Dynamics and Earthquake Engineering, vol. 88, 2016, 76-91.
[9] *Abramowitz M. and Stegun I.A.* (1965), Handbook of mathematical functions, Dover, New York.
[10] *Achenbach J. D.* (1973), Wave propagation in elastic solids, Noth - Holland, Amsterdam.
[11] *Boore D. M.* (1970), Finite-difference solutions to the equations of elastic wave propagation, with applications to Love waves over dipping interfaces; PhD thesis M.I.T.
[12] *Byrne P. M.* (1980), Seismic response of buildings on soft foundation soils, 7th World conference on earthquake engineering, Vol. 6, 29-96.
[13] *Chew W. C. and Wagner R. L.* (1992), A modified form of Liao's absorbing boundary condition, IEEE AP-S/URSI Int. Symp. Dig., Chicago IL, 536-539.
[14] *Clayton R. and Engquist B.* (1977), Absorbing boundary conditions for acoustic and elastic wave equations, BSSA vol. 67, 1529-1540.
[15] *Clearbout J. F. and Johnson A.* (1971), Extrapolation of time dependent wave forms along their path of propagation, Geophysics J. of Royal Astron. Soc, 285-293.
[16] *Engquist B., Majda A.* (1977), Absorbing boundary conditions for the numerical simulation of waves, Math. Comp. 31, 629-651; Univ. of Southern California, Los Angeles, CA.
[17] *Gicev V. and Trifunac M.* (2007), Energy and power of nonlinear waves in seven story reinforced concrete building, Soil Journal of Indian Society of Earthquake Technology, vol.44 (1.1), 305-323.
[18] *Gicev V. and Trifunac M.* (2011), A note on predetermined earthquake damage scenarios for structural health monitoring, Structural control and health monitoring, 19, 746-757.
[19] *Grote M.J. and Keller J.B.* (1996), Nonreflecting boundary conditions for time-dependent scattering, Journal of Computational Physics 127, 52-65.
[20] *Grote M.J. and Kirsch C* (2004), Dirichlet-to-Neumann boundary conditions for multiple scattering problems, Journal of Comput. Phys 201 (6.2), 630-650.
[21] *Grote M.J. and Kirsch C* (2007), Nonreflecting boundary condition for time-dependent multiple scattering, Journal of Comput. Phys 221 (1.1), 41-62.
[22] *Todorovska M, Trifunac M.* (2006), Impulse response analysis of the Van Nuys 7-story hotel during 11 earthquakes (1971-1994): one-dimensional wave propagation and inferences on global and local reduction of stiffness due to earthquake damage, Report CE06-01, Dept. of Civil Eng., University of Southern California, Los Angeles, California.
[23] *Tsynkov S.V.* (1998), Numerical solution of problems on unbounded domains. A review, Applied Numerical Mathematics 27, 465 – 532.
[24] *Waas G.* (1972), Linear two - dimensional analysis of soil dynamic problems in semi - infinite layered media, PhD dissertation.
[25] *Wagner R.L and Chew W.C.* (1995), An analysis of Liao's Absorbing boundary condition; journal of Electromagnetic Waves and Applications vol.9 no. 7- 8, 993-1009.
[26] *Gicev, V. and Trifunac,* M.D. Permanent Deformations and Strains in a Shear Building Excited by a Strong Motion Pulse. Soil Dynamics and Earthquake Engineering, vol. 27, issue 8, August 2007, 774-792.

[27] *Gicev, V. and Trifunac, M.D.* Rotations in a shear beam model of a seven-story building caused by nonlinear waves during earthquake excitation, Structural Control and Health Monitoring, vol. 16 (4),460-482, 2009, Published Online: Jul 8 2008 DOI:10.1002/stc264.
[28] *Gicev, V. and Trifunac, M.D.* Transient and permanent rotations in a shear layer excited by strong earthquake pulses, Bulletin of the Seismological Society of America, vol. 99 (2B), 2009, 1391-1403.
[29] *Gicev, V. and Trifunac, M.D.* Transient and permanent shear strains in a building excited by strong earthquake pulses, Soil Dynamics and Earthquake Engineering, vol. 29, issue 10, 2009, 1358-1366. Published Online: 3 June 2009 DOI: 10.1016/j.soildyn.2009.05.003.
[30] *Gicev, V.* Interakcija tlo-objekat u nelinearnom tlu, Izgradnja, vol. 62, br.12, 2008, 555-566.
[31] *Aviles, J., Suarez, M., & Sanchez-Sesma, F.J.* (2002). Effects of wave passage on the relevant dynamic properties of structures with flexible foundation. Earthq. Eng. and Struct. Dynamics, 31, 139 – 159.
[32] *Fujino, Y., &Hakuno, M.* (1978). Characteristics of elasto-plastic ground motion during an earthquake. Bull. Earthquake Res. Institute 53, 359 – 378.
[33] *Fah D.J.* (1992). A hybrid technique for the estimation of strong ground motion in sedimentary basins. Dissertation, Swiss Federal Institute of Technology, Zurich, Switzerland.
[34] *VW Lee, MD Trifunac* (2010) Rocking strong earthquake accelerations, Soil Dynamics and Earthquake Engineering 6 (2), 75-89.
[35] *M. A. Dablain* (1986). "The application of high-order differencing to the scalar wave equation". Geophysics, 51(1), 54-66.
[36] *MD Trifunac, AG Brady* (1975), Correlations of peak acceleration, velocity and displacement with earthquake magnitude, distance and site conditions, Earthquake Engineering & Structural Dynamics 4 (5), 455-471.
[37] *V. Gicev, M.D. Trifunac.* Amplification of linear strain in a layer excited by a shear-wave earthquake pulse, *Soil Dynamics and Earthquake Engineering,* vol. 30, issue 10, 2010, 1073-1081.
[38] *Risteska, Aleksandra and Gicev, Vlado and Zlatev, Zoran and Kokalanov, Vasko* (2013) *The response of a shear beam as 1d medium to seismic excitations dependent on the boundary conditions*. In: XI Balkan Conference on Operation Research, 7-11 Sept 2013, Belgrade & Zlatibor, Serbia.
[39] *V. Gicev*. Soil Structure Interaction in Nonlinear Soil, chapter in the book "Coupled site and Soil-Structure Interaction Effects with Application to Seismic Risk Mitigation", Springer, 2009.
[40] *Josif Josifovski*, Dissertation "Investigation of Soil-Structure interaction using Perfectly Matched Layer as an absorbing boundary condition", Skopje 2010.

Aleksandra Risteska-Kamcheski
University of Goce Delcev, Stip,
Republic of North Macedonia
Faculty of Computer Science
E-mail address: aleksandra.risteska@ugd.edu.mk

Vlado Gicev
University of Goce Delcev, Stip,
Republic of North Macedonia
Faculty of Computer Science
E-mail address: vlado.gicev@ugd.edu.mk